Acta Cryst. (1997). A53, 649–662

Dynamical Diffraction in Periodic Multilayers

V. F. Sears

Atomic Energy of Canada Limited, Chalk River Laboratories, Chalk River, Ontario, Canada K0J 1J0. E-mail: searsv@aecl.ca

(Received 15 November 1996; accepted 23 April 1997)

Abstract

Exact reflectivity curves are calculated numerically for various periodic multilayers using the optical matrix method in order to test the dynamical theory of diffraction. The theory is generally valid for values of the bilayer thickness d up to about 100 Å. For somewhat larger values of d, where the theory begins to break down, the initial discrepancy is in the phase of the oscillations in the wings of the peaks. For very large values of d, where the first-order Bragg peak approaches the edge of the mirror reflection, two general types of multilayers can be distinguished. In the first (typified in the present work by Ni/Ti), there is a large (30% or more) reduction in the actual value of the critical wave vector for total reflection while, in the second (typified here by Fe/Ge), there is very little reduction (3% or so). The origin of these two very different types of behavior is explained. It is also shown that, within the dynamical theory of diffraction, the change in the position of the center of the Darwin plateau as d is varied obeys a universal scaling law – universal in the sense that it is the same for all layer materials and all orders of reflection. The width of the Darwin plateau also obeys a universal scaling law. It is verified that the values of the center and width of the Darwin plateau calculated from the optical matrix method for Ni/Ti and Fe/Ge multilayers obey these scaling laws for a wide range of parameters.

1. Introduction

The reflection of thermal neutrons from an ideal multilayer (*i.e.* a sequence of homogeneous layers separated by plane-parallel boundaries) is an exactly solvable problem in quantum mechanics. Within each layer, the wave function is a superposition of a transmitted wave and a reflected wave. The wave vectors are determined by the kinematics (energy and momentum conservation) and the amplitudes by matching the values of the wave function and its derivative at each boundary. The final result is that the reflectivity can be expressed in terms of a product of known 2×2 matrices, one for each boundary. This 'optical-matrix' method (Heavens, 1965; Jacobsson, 1966; Born & Wolf, 1975; Lekner, 1987) therefore permits an exact numerical calculation of the reflectivity curve for any specified multilayer. For example, Fig. 1 shows the calculated reflectivity of a periodic Ni/Ti multilayer as a function of the normal component of the wave-vector transfer q_z. The calculation is for 50 bilayers, each 200 Å thick, in which the individual Ni and Ti layers have equal thickness.

Although the optical-matrix method is exact, it has no interpretive power. It is simply an algorithm for generating the reflectivity curve of a specified multilayer. It cannot tell us why this curve has the shape that it has or what its features mean physically. In Fig. 1, for example, why does the reflectivity consist of a series of almost equally spaced peaks? Why is the separation of these peaks approximately $2\pi/d$, where d is the bilayer thickness? Why is the separation not exactly $2\pi/d$? Why is the $m = 1$ peak so broad? Why is the $m = 2$ peak so weak? What is the origin of the rapid oscillations in the wings of the peaks? To answer such questions, we need a theory, if only approximate, that highlights the underlying physics.

A periodic multilayer is analogous to a one-dimensional crystal and anyone familiar with X-ray or neutron crystallography will immediately recognize that the peaks in Fig. 1 are due to Bragg reflection. The detailed structure of the Bragg peaks in a perfect crystal is described by the dynamical theory of diffraction, in which the wave function inside the crystal is represented by a coherent superposition of Bloch waves (Ewald, 1917; von Laue, 1931; Zachariasen, 1945; Sears, 1989). The success of the dynamical theory of diffraction lies in the existence of a small parameter in terms of which the wave vectors and amplitudes can be expanded. This parameter is defined as

$$\xi = (q_0/q_z)^2, \tag{1}$$

where q_0 is the critical wave vector for total mirror reflection. Keeping only the leading terms in the above-mentioned expansions, one obtains a simple analytical formula for the reflectivity in terms of which questions such as those posed earlier can be answered.

In general, $q_0 \simeq 0.01$ Å^{-1} and, for a crystal, d is somewhat smaller than the lattice constant so that $\xi \simeq 10^{-5}$ to 10^{-6} for a first-order Bragg peak. As a result, the dynamical theory of diffraction for a perfect

crystal is essentially exact for all practical purposes. For a multilayer, on the other hand, d is typically one or two orders of magnitude larger than the lattice constant and $\xi \simeq 0.01$ to 1.0. In this case, the dynamical theory of diffraction can be expected to be valid only when the bilayers are very thin and to break down when they become sufficiently thick.

In this present paper, we use exact reflectivity curves, calculated numerically from the optical-matrix method for various ideal multilayers, to test the dynamical theory of diffraction. We find, for example, that the theory is generally valid for values of d up to about 100 Å. For somewhat larger values of d, where the theory begins to break down, the initial discrepancy is in the phase of the oscillations in the wings of the peaks. For very large values of d, where the first-order Bragg peak (labeled $m = 1$ in Fig. 1) approaches the edge of the mirror reflection ($m = 0$), one can distinguish two general types of multilayers. In the first (typified in the present work by Ni/Ti), there is a large (30% or more) reduction in the actual value of the critical wave vector for total reflection while, in the second (typified here by Fe/Ge), there is very little reduction (3% or so). The origin of these two very different types of behavior is explained.

The flat part of the $m = 1$ Bragg peak in Fig. 1 is generally called the Darwin plateau. We show that, within the dynamical theory of diffraction, the change in the position of the center of the Darwin plateau as d is varied obeys a universal scaling law - universal in the sense that it is the same for all layer materials and all values of m. The width of the Darwin plateau also obeys a universal scaling law. We verify that the values of the center and width of the Darwin plateau calculated from the optical-matrix method for Ni/Ti and Fe/Ge multilayers obey these scaling laws for a wide range of d and m values.

We begin in §2 with a brief derivation of the dynamical theory of diffraction for an ideal periodic multilayer. Although the theory is essentially the same as for a perfect crystal, it differs in the definitions of many of the quantities involved. Most of the mathematical details are put in Appendices at the end of the paper. In §3, we show that, in a first approximation, the

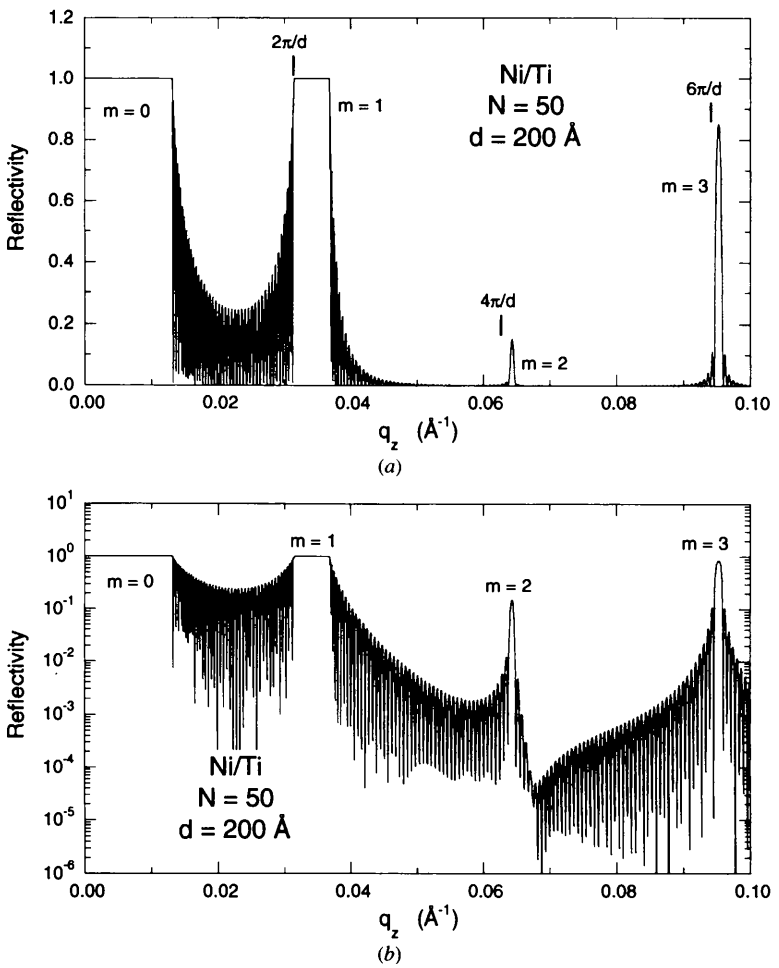

Fig. 1. Reflectivity of a periodic Ni/Ti multilayer as a function of q_z calculated exactly using the optical-matrix method and shown on (*a*) linear and (*b*) logarithmic scales. The dominant features are the mirror reflection ($m = 0$) and the first three Bragg peaks ($m = 1, 2, 3$), which are separated by oscillating wings. The positions of the reciprocal-lattice vectors $2\pi m/d$ are indicated by vertical lines in (*a*).

reflectivity of the mirror reflection peak is the same as Airy's formula for reflection from a single homogeneous layer whose thickness is the same as the total thickness of the multilayer. In §4, we obtain the basic formula for the reflectivity of the Bragg peaks and discuss some of its general properties. Finally, in §5, we present a detailed numerical comparison of the main results from the dynamical theory of diffraction with the corresponding exact results for Ni/Ti and Fe/Ge multilayers calculated from the optical-matrix method.

2. Dynamical diffraction in a periodic multilayer

In previous discussions of the reflectivities of multilayer neutron monochromators, the validity of the dynamical theory of diffraction has always been taken for granted (Saxena & Schoenborn, 1975, 1977; Sears, 1983; Saxena, 1986). The authors have simply transcribed the standard formula for the reflectivity of a perfect crystal to the case of a periodic multilayer without verifying whether the theory is valid for the d values of interest. In fact, the bilayer thicknesses are typically in the range 30 to 300 Å and it will be seen later that the dynamical theory of diffraction usually breaks down in the upper half of this range. It is therefore worthwhile to begin by driving the dynamical theory of diffraction for the explicit case of a periodic multilayer, with particular emphasis on the approximations that are made and their range of validity. Our treatment has been adapted from that given in the book by Sears (1989).

2.1. *Wave equation for a periodic multilayer*

The coherent wave $\psi(\mathbf{r})$, which describes the coherent elastic scattering of thermal neutrons in macroscopic media and, hence, all neutron-optical phenomena, satisfies a one-body wave equation

$$\{(-\hbar^2/2m)\Delta + V(\mathbf{r})\}\psi(\mathbf{r}) = E\psi(\mathbf{r}), \tag{2}$$

in which m is the neutron mass, E the incident-neutron energy and $V(\mathbf{r})$ the optical potential that represents the effective interaction of the neutron with the system. To a good approximation, the optical potential is given by the equilibrium value of the Fermi pseudopotential,

$$V(\mathbf{r}) = (2\pi\hbar^2/m)f(\mathbf{r}). \tag{3}$$

Here, $f(\mathbf{r}) = \rho(\mathbf{r})b(\mathbf{r})$ is the bound coherent scattering-length density, in which $\rho(\mathbf{r})$ is the average number of atoms per unit volume at the point $\mathbf{r}$ and $b(\mathbf{r})$ the corresponding average bound coherent scattering length per atom.

We consider the reflection of neutrons by an ideal multilayer consisting of N identical bilayers of thickness d. The z direction will be taken normal to the surface so that $f(\mathbf{r}) = f(z)$, independent of x and y. Inside the multilayer, $f(z)$ is a periodic function of z with period d and, hence, can be expanded as a Fourier series in this region. Ignoring the substrate, we can therefore put

$$f(z) = \begin{cases} 0, & z < 0, \\ \sum_m f_m \exp(-iK_m z), & 0 < z < D, \\ 0, & z > D, \end{cases} \tag{4}$$

where $D = Nd$ is the total thickness of the multilayer. The quantities K_m are defined as

$$K_m = 2\pi m/d, \quad m = 0, \pm 1, \pm 2, \ldots, \tag{5}$$

and are analogous to reciprocal-lattice vectors, while the coefficients f_m are analogous to unit-cell structure factors. Explicit expressions for f_m are given in Appendix A for some model bilayers.

Since the scattering-length density depends only on z, the solution of the wave equation (2) is of the form

$$\psi(\mathbf{r}) = \exp[i(k_x x + k_y y)]\chi(z), \tag{6}$$

where k_x and k_y are constants. In other words, momentum is conserved in the x and y directions. Defining k_z^2 such that

$$E = (\hbar^2/2m)(k_x^2 + k_y^2 + k_z^2), \tag{7}$$

we then find that $\chi(z)$ satisfies the one-dimensional wave equation

$$\{d^2/dz^2 + k_z^2 - 4\pi f(z)\}\chi(z) = 0. \tag{8}$$

Let us choose coordinate axes such that the plane of scattering is the xz plane. Then, $k_y = 0$ and the incident and reflected wave vectors are given by

$$\begin{aligned} \mathbf{k} &= (k_x, k_y, k_z) = k(\cos\theta, 0, \sin\theta), \\ \mathbf{k}' &= (k_x, k_y, -k_z) = k(\cos\theta, 0, -\sin\theta), \end{aligned} \tag{9}$$

where θ is the angle that the incident wave vector makes with the surface. The wave-vector transfer is therefore given by

$$\mathbf{q} = \mathbf{k} - \mathbf{k}' = (0, 0, q_z), \tag{10}$$

where

$$q_z = 2k_z = 2k\sin\theta = (4\pi/\lambda)\sin\theta \tag{11}$$

and $\lambda = 2\pi/k$ is the incident-neutron wavelength.

2.2. *General solution of the wave equation*

With $f(z)$ of the form (4), the required solution of (8) can be expressed as

$$\chi(z) = \begin{cases} \exp(ik_z z) + r\exp(-ik_z z), & z < 0, \\ \sum A(z)\exp(iK_z z), & 0 < z < D, \\ t\exp(ik_z z), & z > D. \end{cases} \tag{12}$$

In the region $z < 0$, the wave function is a superposition of an incident wave, which is normalized to unit amplitude, and a reflected wave with relative amplitude r. For $z > D$, we have a transmitted wave with relative

amplitude t. In the interior of the multilayer, where $0 < z < D$, the wave function is a superposition of Bloch waves in which the sum runs over all allowed values of K_z, which are determined by the wave equation as shown below.

The reflectivity R is defined as the fraction of incident neutrons that are reflected by the multilayer and the transmissivity T as the fraction that are transmitted. These quantities are given by

$$R = |r|^2, \quad T = |t|^2. \tag{13}$$

To determine R and T, we must therefore solve the wave equation (8) for the interior wave function and then match it to the exterior solutions by requiring that $\chi(z)$ and $\chi'(z)$ be continuous at $z = 0$ and $z = D$.

The Bloch-wave amplitude $A(z)$ is a periodic function of z with period d and, hence, can be expanded as a Fourier series

$$A(z) = \sum_m A_m \exp(-iK_m z). \tag{14}$$

For each allowed value of K_z, the interior wave function is then of the form

$$\chi(z) = A(z)\exp(iK_z z) = \sum_m A_m \exp[i(K_z - K_m)z]. \tag{15}$$

This expression satisfies the wave equation (8) if and only if

$$D_m A_m = \xi \sum_{m'} \hat{f}_{m-m'} A_{m'}. \tag{16}$$

Here,

$$D_m = 1 - [(K_z - K_m)/k_z]^2 \tag{17}$$

and

$$\hat{f}_m = f_m/f_0, \tag{18}$$

so that $\hat{f}_0 = 1$. Also,

$$\xi = 4\pi f_0/k_z^2 = (q_0/q_z)^2, \tag{19}$$

in which $q_z = 2k_z$ as before and

$$q_0^2 = 16\pi f_0. \tag{20}$$

We shall see in the next section that q_0 is the critical wave vector for mirror reflection from the multilayer.

2.3. *General form of the reflectivity*

The fundamental assumption in the dynamical theory of diffraction is that ξ is a small parameter in terms of which expansions can be made. In what follows, $a \simeq b$ is to be interpreted as $a = b[1 + O(\xi)]$, while $a \neq b$ means that the relative difference between a and b is of order unity.

For example, we shall see later that $K_z \simeq k_z$, which gives

$$D_m = 4K_m(q_z - K_m)/q_z^2 + O(\xi). \tag{21}$$

Also, according to (16),

$$D_m A_m = O(\xi). \tag{22}$$

Thus, if $q_z \simeq K_m$ then

$$D_m = O(\xi), \quad A_m = O(1), \tag{23}$$

while if $q_z \neq K_m$ then

$$D_m = O(1), \quad A_m = O(\xi). \tag{24}$$

Note that if $q_z = K_m$ exactly then it follows from (5) and (11) that

$$m\lambda = 2d\sin\theta, \tag{25}$$

which is just Bragg's law.

It is clear from the above discussion that the nature of the wave function depends critically on the value of q_z relative to K_m. The basic procedure in the dynamical theory of diffraction is to neglect all terms in the interior wave function (15) for which $A_m = O(\xi)$. In subsequent sections, we show that the reflectivity then consists of a series of distinct peaks when viewed as a function of q_z:

$$R = \sum_m R_m. \tag{26}$$

Here, R_m arises from Bragg reflection *via* K_m and is appreciably different from zero only if $q_z \simeq K_m$. The leading term R_0 arises from mirror reflection and is appreciably different from zero only at small q_z.

3. Mirror reflection

3.1. *Reflectivity*

In Appendix B, it is shown that, when Bragg's law is not satisfied for any value of $m \neq 0$, the reflectivity of a multilayer is the same as for a single homogeneous layer of thickness D and scattering-length density f_0 and can be expressed in the form

$$R_0 = R_0(x_0, y_0), \tag{27}$$

where x_0 and y_0 are dimensionless variables that characterize the wave-vector transfer and the thickness of the multilayer, respectively,

$$x_0 = q_z/q_0, \quad y_0 = q_0 D/2, \tag{28}$$

and q_0 is given by (20). Alternatively,

$$y_0 = \pi N/N_0, \tag{29}$$

where N is the number of bilayers and

$$N_0 = 2\pi/q_0 d. \tag{30}$$

In what follows, we shall neglect absorption by assuming that f_0 is real. We shall also assume that f_0 is positive, which it usually is in practice. In this case, q_0 and, hence, x_0 and y_0 are also real positive quantities. Finally, dropping the subscripts on the variables,

$$R_0(x, y) = \left|2x^2 - 1 + 2ix(x^2 - 1)^{1/2} \cot[y(x^2 - 1)^{1/2}]\right|^{-2}, \tag{31}$$

and this is equivalent to Airy's formula (Born & Wolf, 1975). Fig. 2 shows $R_0(x, y)$ as a function of x for three values of y.

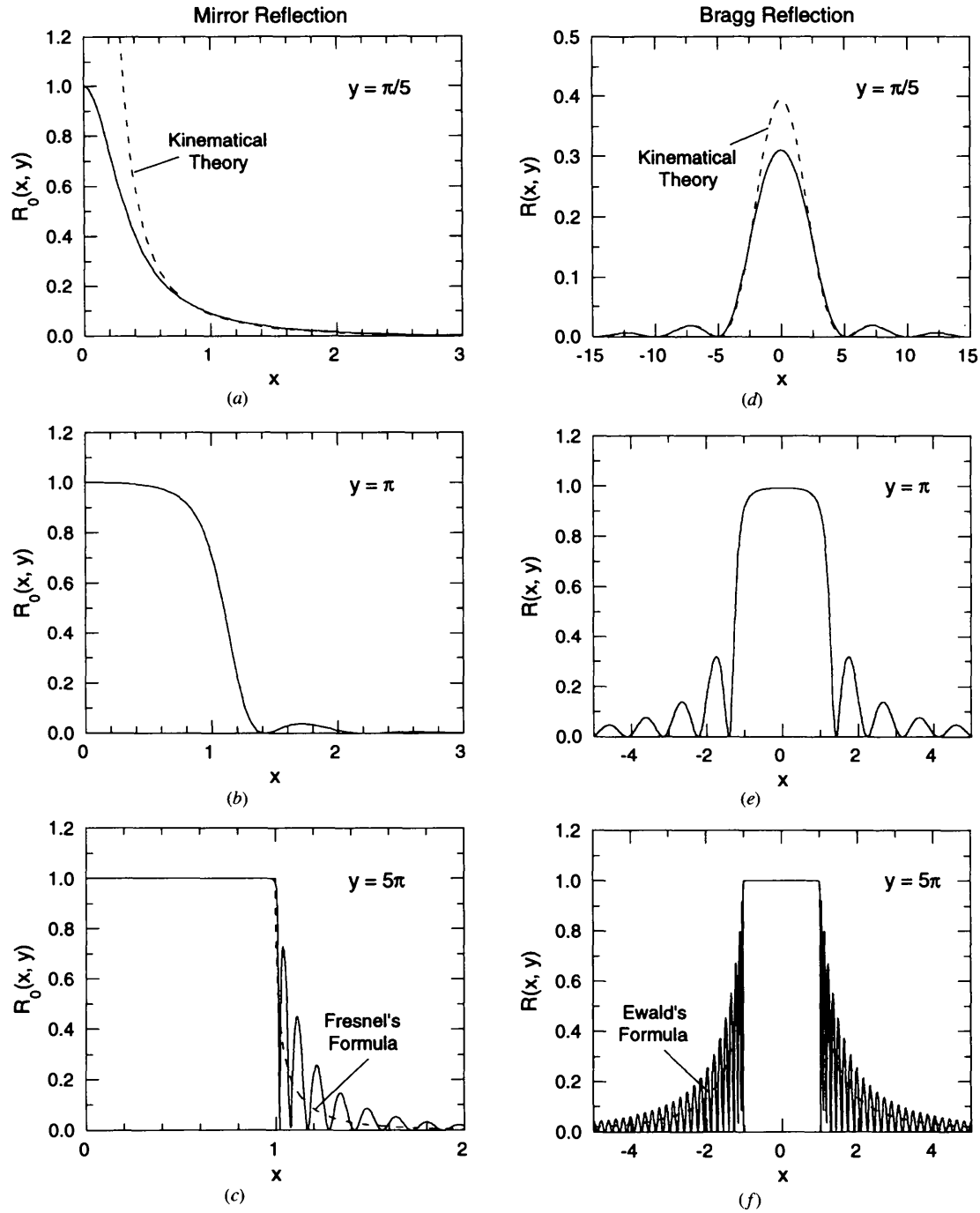

Fig. 2. The functions $R_0(x, y)$ and $R(x, y)$ that characterize mirror reflection and Bragg reflection in the dynamical theory of diffraction, shown here as functions of x for three values of y.

3.2. *Properties of the reflectivity*

It will be noted from the general expression (31) that

$$R_0(x,y) = \begin{cases} 1, & x = 0, \\ y^2/(y^2+4), & x = 1, \\ 0, & x = \infty. \end{cases} \quad (32)$$

Also,

$$R_0(x,\infty) = 1, \quad 0 \le x \le 1. \quad (33)$$

It is evident from Fig. 2(*c*) that, for practical purposes, this latter relation is valid when $y \gg \pi$ and that $R_0(x,y)$ decreases rapidly to zero when $x > 1$. Since the boundary $x = 1$ occurs when $q_z = q_0$, it follows that q_0 is the critical wave-vector transfer for total reflection from a thick multilayer. The quantity N_0 in (29) is essentially the number of bilayers needed to saturate the reflectivity. In Fig. 1, for example, $N_0 = 2.29$ and $y_0 = 22\pi$ so that the mirror reflection is well saturated.

For a thin multilayer ($y \ll \pi$), (31) reduces to

$$R_0(x,y) = (\sin xy/2x^2)^2, \quad (34)$$

which is the same as is found in the kinematical theory of diffraction (Sears, 1988). This result is shown by the dashed line in Fig. 2(*a*). Since the kinematical theory neglects multiple scattering, it is valid only if $R_0 \ll 1$. This condition is not well satisfied when x is very small ($x < 0.6$, say).

It is instructive to compare (31) for reflection from a multilayer of finite thickness with Fresnel's formula for reflection from a homogeneous medium of infinite thickness (Born & Wolf, 1975),

$$R_F(x) = \left|[(x^2-1)^{1/2} - x]/[(x^2-1)^{1/2} + x]\right|^2. \quad (35)$$

This latter result is shown by the dashed line in Fig. 2(*c*). It is clear from the wave function (69) that the oscillations in the tail of $R_0(x,y)$ above $x = 1$ are due to the interference of the wave reflected from the back face of the multilayer with the internal transmitted wave.

4. Bragg reflection

4.1. *Reflectivity*

In Appendix *C*, it is shown that, when Bragg's law is satisfied for some value of $m \neq 0$, the reflectivity of a non-absorbing multilayer is of the form

$$R_m = R(x_m, y_m), \quad (36)$$

where x_m and y_m are dimensionless variables that characterize the wave-vector transfer and the thickness of the multilayer, respectively,

$$x_m = [2K_m(q_z - K_m) - q_0^2]/q_m^2, \quad y_m = q_m^2 D/4K_m. \quad (37)$$

Here, q_0 is given by (20) as before and

$$q_m^2 = 16\pi|f_m|. \quad (38)$$

Alternatively,

$$y_m = \pi N/N_m, \quad (39)$$

where N is again the number of bilayers and

$$N_m = 8\pi^2 m/(q_m d)^2. \quad (40)$$

Finally, dropping the subscripts on the variables,

$$R(x,y) = \frac{\sin^2[y(x^2-1)^{1/2}]}{x^2 - 1 + \sin^2[y(x^2-1)^{1/2}]}. \quad (41)$$

Fig. 2 shows $R(x,y)$ as a function of x for three values of y.

It will be noted that R_m depends on m only through the variables x_m and y_m. The intrinsic shape of a Bragg peak is given by the function $R(x,y)$, which is independent of m. In other words, all the Bragg peaks have the same shape. In the neighbourhood of the Bragg peak, the expansion parameter (19) becomes

$$\xi = (q_0/q_z)^2 \simeq (q_0/K_m)^2. \quad (42)$$

The dynamical theory of diffraction is valid only if $\xi \ll 1$, which requires that $K_m \gg q_0$.

4.2. *Properties of the reflectivity*

It will be noted from the general expression (41) that

$$R(x,y) = \begin{cases} \tanh^2 y, & x = 0, \\ y^2/(y^2+1), & x = \pm 1, \\ 0, & x = \pm\infty. \end{cases} \quad (43)$$

Also,

$$R(x,\infty) = 1, \quad 0 \le x^2 \le 1. \quad (44)$$

It is evident from Fig. 2(*f*) that, for practical purposes, this latter relation is valid when $y \gg \pi$ and that $R(x,y)$ decreases rapidly to zero when $x^2 > 1$. The region of total reflectivity is called the Darwin plateau (Darwin, 1914), and the quantity N_m in (39) is essentially the number of bilayers needed to saturate the reflectivity. For the $m = 1$ Bragg peak in Fig. 1, for example, $N_1 = 10.85$ and $y_1 = 4.6\pi$ so that the Darwin plateau is well saturated. However, for the $m = 3$ Bragg peak, $N_3 = 97.7$ and $y_3 = 0.5\pi$ so that the peak is not saturated and there is no well defined Darwin plateau.

For a thin multilayer ($y \ll \pi$), (41) reduces to

$$R(x,y) = [(\sin xy)/x]^2, \quad (45)$$

which is the same as is found in the kinematical theory of diffraction (Sears, 1983). The term $-(q_0/q_m)^2$ in (37) for x_m is absent in the kinematical theory and R_m is symmetric about the Bragg position $q_z = K_m$. In the dynamical theory, the effect of this term is that the Bragg peak is not centered at $q_z = K_m$ (see Fig. 1),

although the shift is only appreciable at large y. The kinematical limit (45) is shown by the dashed line in Fig. 2(*d*). Since the kinematical theory neglects multiple scattering, it is valid only if $R(x, y) \ll 1$. This condition is not well satisfied when x is very small ($x < 2$, say) and the reduction in the intensity of the peak in Fig. 2(*d*) is referred to as extinction.

4.3. *Darwin plateau*

The boundaries of the Darwin plateau occur at $x = \pm 1$, where q_z has the values

$$Q_{m\pm} = K_m + (q_0^2 \pm q_m^2)/2K_m. \tag{46}$$

Hence, the center of the plateau is at

$$Q_m = \tfrac{1}{2}(Q_{m+} + Q_{m-}) = K_m + q_0^2/2K_m \tag{47}$$

and its width is given by

$$\Delta Q_m = Q_{m+} - Q_{m-} = q_m^2/K_m. \tag{48}$$

It is easily seen, with the help of (68), that $Q_m n_z = K_m$ to first order in ξ. In other words, the center of the Darwin plateau occurs where the refracted wave-vector transfer equals the reciprocal-lattice vector. Thus, the shift of the center of the Bragg peak from the kinematical position $Q_m = K_m$ is due to the refraction of the wave function inside the multilayer. Such shifts have been observed in multilayer neutron monochromators (Ebisawa, Achiwa, Yamada, Akiyoshi & Okamoto, 1979; Gukasov *et al.*, 1979). The analogous deviation from Bragg's law for crystals is well known and was first established by Darwin (1914).

Note also that the minimum value of Q_m is $2^{1/2}q_0$ and occurs at $K_m = q_0/2^{1/2}$. This result is, however, of purely academic interest since the dynamical theory of diffraction is only valid when $\xi \ll 1$, which, according to (42), means only when $K_m \gg q_0$.

The rapid oscillations in the wings of $R(x, y)$ when $y \gg \pi$ arise from the interference of the $\pm$ components in the wave function (95) and are referred to as *Pendellösung* oscillations. If we average (41) over these oscillations, we get Ewald's formula (Ewald, 1917):

$$\bar{R}(x) = \begin{cases} 1, & x^2 \le 1, \\ 1 - (1 - x^{-2})^{1/2}, & x^2 > 1. \end{cases} \tag{49}$$

This latter result is shown by the dashed line in Fig. 2(*f*).

5. Application to Ni/Ti and Fe/Ge multilayers

We mentioned in §1 that the reflectivity of an ideal multilayer can be calculated exactly using the well known optical-matrix method. In this section, we compare the results of such calculations for periodic Ni/Ti and Fe/Ge multilayers with the corresponding results obtained from the dynamical theory of diffraction. The optical-matrix method can be formulated in a number of equivalent ways. We have used an approach that is originally due to Abelès (1948). A very readable account of this method can be found in Lekner (1987).

Table 1. *Properties of selected layer materials*

	ρ (Å^{-3})	b (fm)	f (10^{-6} Å^{-2})
Ni	0.0914	10.30	9.42
Ti	0.0567	−3.44	−1.95
Fe	0.0849	9.45	8.02
Ge	0.0441	8.19	3.61

Table 2. *Properties of two symmetric multilayers*

	f_0 (10^{-6} Å^{-2})	$\lvert f_1\rvert$ (10^{-6} Å^{-2})	q_0 (Å^{-1})	q_1 (Å^{-1})	q_1/q_0
Ni/Ti	3.73	3.62	0.0137	0.0135	0.985
Fe/Ge	5.82	1.40	0.0171	0.0084	0.491

The relevant properties of the layer materials are listed in Table 1. We use the bulk values for the number density ρ, ignoring the fact that in actual thin films the density can be as much as 10% smaller than the bulk values (Ebisawa *et al.*, 1979). We also assume symmetric bilayers (see Appendix *A*) and the corresponding values of q_0 and q_m for $m = 1$ are given in Table 2. Note that $q_0 \simeq q_1$ for Ni/Ti while q_0 is a factor of two larger than q_1 for Fe/Ge. This will be seen later to lead to an important qualitative difference in the behavior of the reflectivity in thick multilayers.

5.1. *Reflectivity curves*

Fig. 3 shows the reflectivity curves for mirror reflection in periodic Ni/Ti and Fe/Ge multilayers for three values of the bilayer thickness d. In all cases, the number of bilayers N was chosen large enough to saturate the reflectivity below the critical wave vector. The solid curves are exact results calculated using the optical-matrix method while the dashed curves are from dynamical diffraction theory (see §3). We see that the results are in excellent agreement in Ni/Ti for values of d up to about 50 Å and in Fe/Ge up to about 100 Å. For larger values of d, the initial discrepancy is in the phase of the oscillations in the tails of the reflectivity curves.

Fig. 4 shows the corresponding results for the first-order Bragg reflection in these multilayers (see §4). For both multilayers, there is excellent agreement for values of d up to about 100 Å. For larger values of d, the Bragg peaks obtained from dynamical diffraction theory are noticeably shifted to larger values of q_z relative to those obtained from the exact calculations and there are also large discrepancies in the wings of the distributions. According to (42),

$$\xi \simeq (q_0 d/2\pi m)^2 \tag{50}$$

and the dynamical theory of diffraction is valid only if $\xi \ll 1$. In general, this requires that d be sufficiently small and/or m sufficiently large. For the same values of

d and m, the parameter ξ is larger for Fe/Ge than for Ni/Ti because q_0 is larger (see Table 2).

According to (60), the structure factor f_m for a symmetric bilayer vanishes identically when m is even and the corresponding Bragg reflection is forbidden within the dynamical theory of diffraction. In fact, a weak $m = 2$ reflection is present in the exact reflectivity curve for Ni/Ti shown in Fig. 1. This peak is seen to be highly asymmetric, in contrast to those for the allowed reflections $m = 1$ and $m = 3$. The $m = 2$ reflection is, in

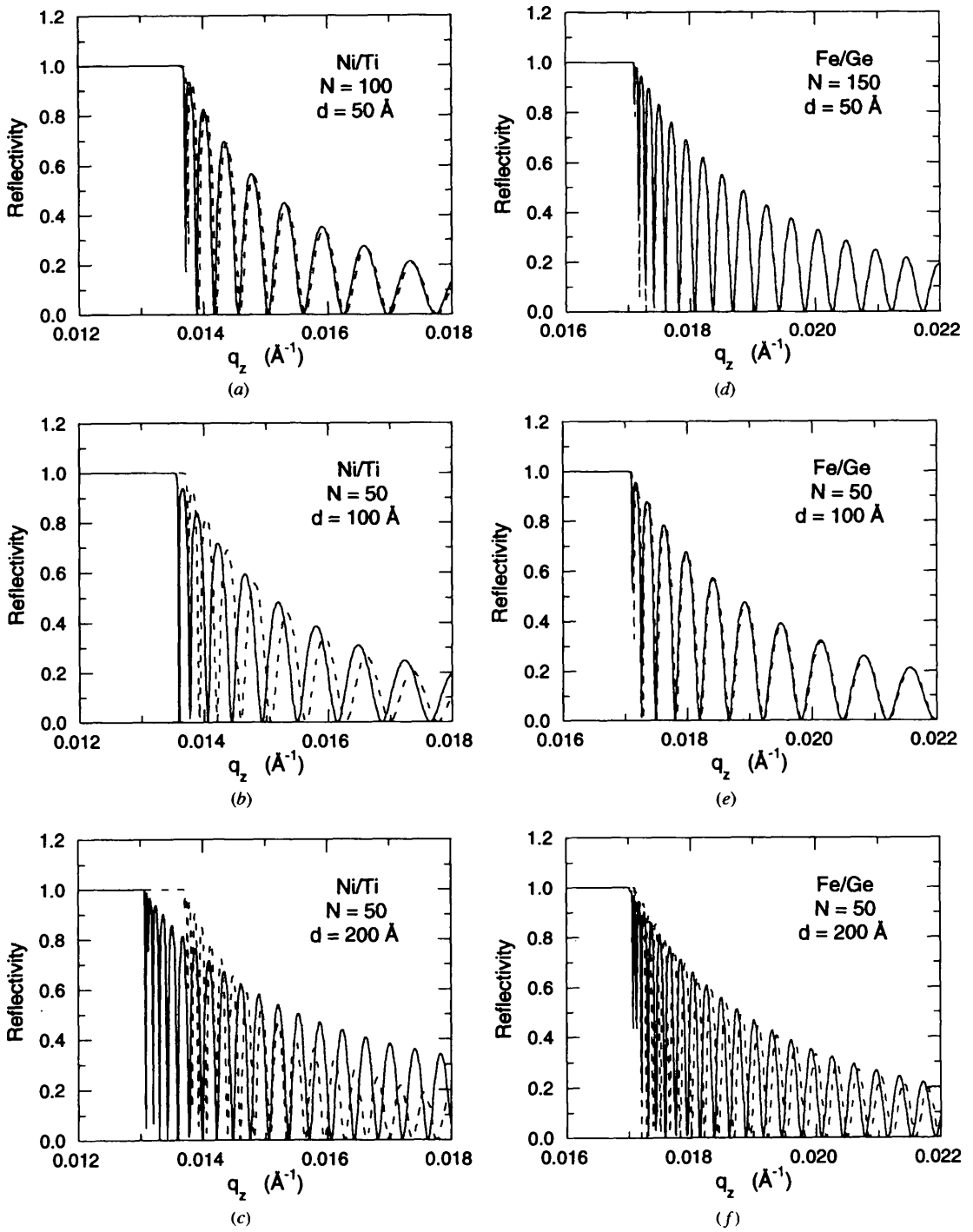

Fig. 3. Mirror reflection in periodic Ni/Ti and Fe/Ge multilayers for three values of the bilayer thickness d. The solid curves are exact results calculated using the optical-matrix method and the dashed curves are from dynamical diffraction theory.

effect, due to the ξ^2 terms in (80) that are normally neglected in the dynamical theory of diffraction. These higher-order terms represent multiple-scattering processes in which, for example, the neutron is first Bragg reflected *via* K_3 and later *via* K_{-1}. The total wave-vector transfer is then $K_3 + K_{-1} = K_2$. In this way, the otherwise forbidden $m = 2$ reflection becomes active. This is, of course, just the analog of the Renninger

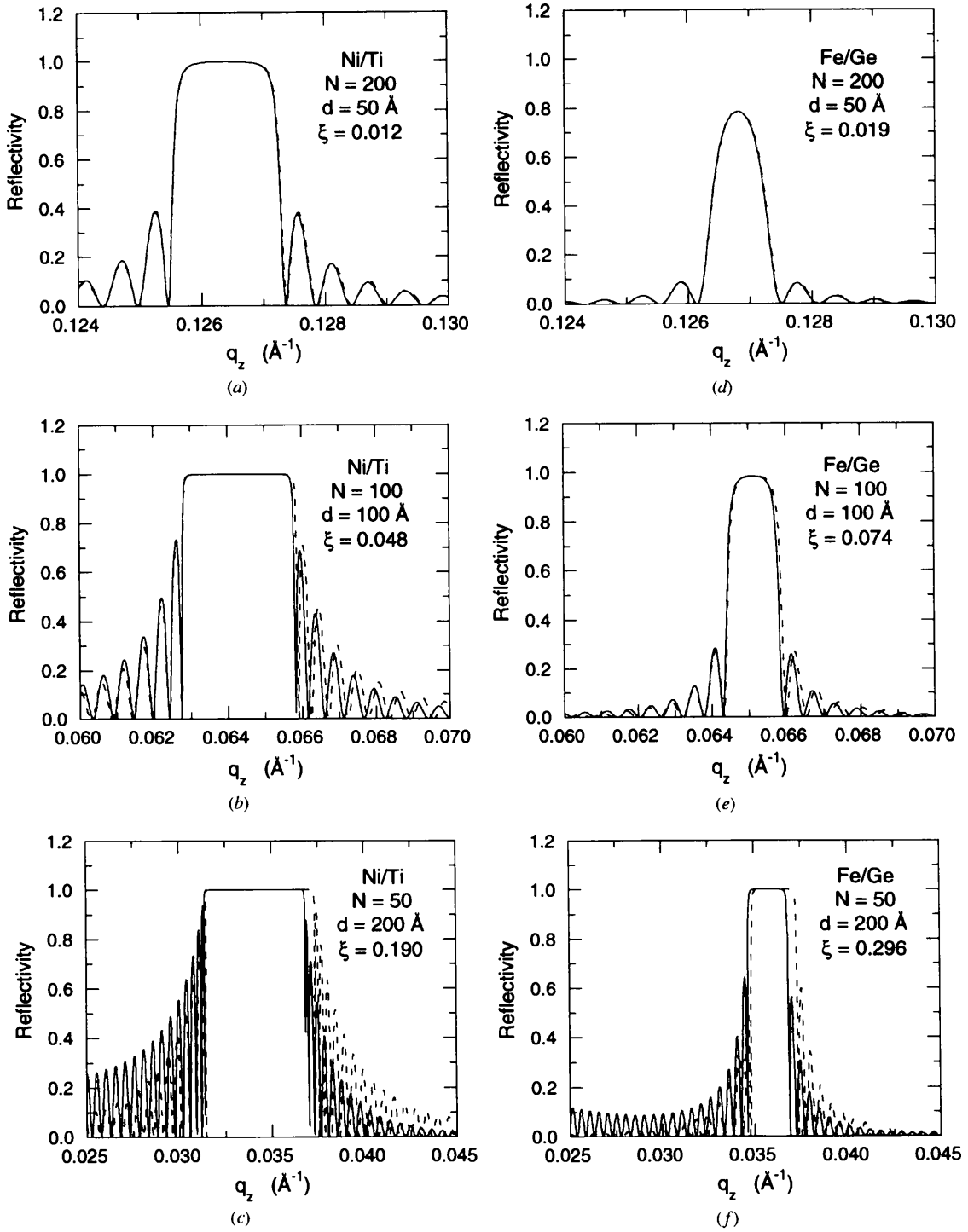

Fig. 4. First-order Bragg peaks in periodic Ni/Ti and Fe/Ge multilayers for three values of the bilayer thickness d. The solid curves are exact results calculated using the optical-matrix method and the dashed curves are from dynamical diffraction theory.

effect in Bragg reflection in perfect crystals (Renninger, 1937).

5.2. *Critical wave vectors*

Fig. 5 shows the critical wave vectors for a periodic Ni/Ti multilayer as functions of the bilayer thickness d. In particular, the dashed line represents q_0, which is the critical wave vector for mirror reflection in dynamical diffraction theory, and the solid curves show the quantities $Q_{m\pm}$, which mark the edges of the Darwin plateau for each allowed value of m. The circles are the corresponding exact positions of the total reflection edges that were read from reflectivity curves calculated for thick multilayers using the optical-matrix method. The most notable discrepancies are for $m = 0$ and 1 when $d > 200$ Å. The corresponding results for Fe/Ge are shown in Fig. 6.

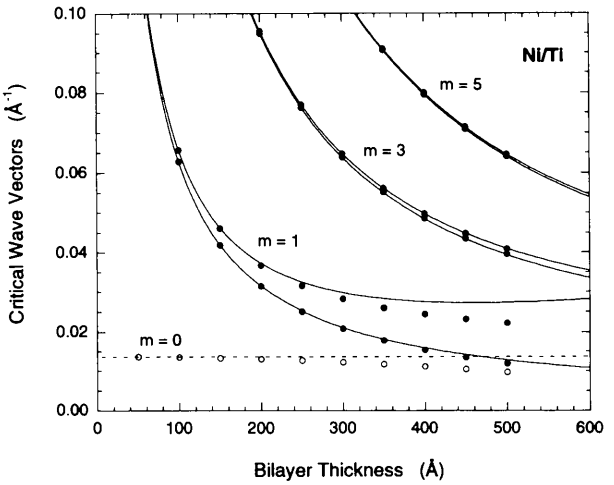

Fig. 5. Critical wave vectors q_0 (dashed line) and $Q_{m\pm}$ (solid curves) for a periodic Ni/Ti multilayer given by dynamical diffraction theory and shown here as functions of the bilayer thickness d. The circles are the corresponding exact positions of the total reflection edges calculated using the optical-matrix method.

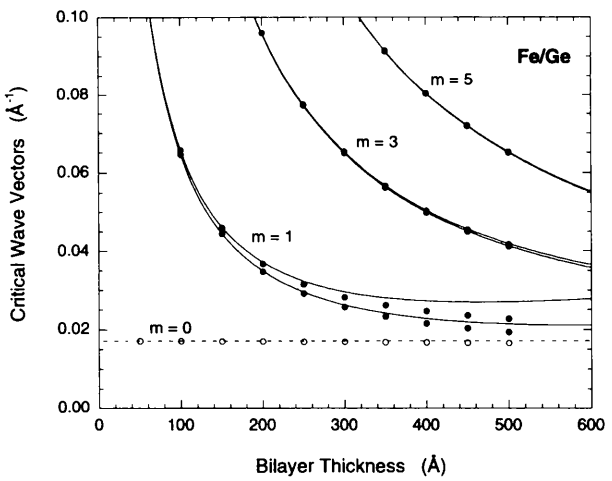

Fig. 6. Critical wave vectors q_0 (dashed line) and $Q_{m\pm}$ (solid curves) for a periodic Fe/Ge multilayer given by dynamical diffraction theory and shown here as functions of the bilayer thickness d. The circles are the corresponding exact positions of the total reflection edges calculated using the optical-matrix method.

According to (46), the lower edge of the first-order Darwin plateau intersects the critical wave vector for mirror reflection (in other words, $Q_{1-} = q_0$) when

$$K_1 = 2\pi/d = \tfrac{1}{2}[q_0 + (2q_1^2 - q_0^2)^{1/2}]. \qquad (51)$$

Since K_1 is real, this requires that

$$q_1/q_0 \geq 1/2^{1/2} = 0.7071. \qquad (52)$$

This condition is satisfied for Ni/Ti, where $q_1/q_0 = 0.985$ (see Table 2) and the lower edge of the Darwin plateau intersects the mirror reflection line at $d = 465$ Å (see Fig. 5). It is seen from the open circles in Fig. 5 that, in reality, the mirror reflection edge is depressed as the Bragg peak approaches it so that the two never actually meet. This is illustrated in Fig. 7, which shows the reflectivity of Ni/Ti as a function of q_z calculated at $d = 450$ Å using the optical-matrix method. For this value of d, the reciprocal-lattice vector $2\pi/d$ is almost equal to q_0 and the mirror reflection edge is depressed by about 25%.

The condition (52) is not satisfied for Fe/Ge, where $q_1/q_0 = 0.491$ (see Table 2), so that the Darwin plateau does not intersect the mirror reflection line (see Fig. 6). It is evident from the open circles in this figure that the critical wave vector for mirror reflection remains within 3% of the value q_0 given by the dynamical theory of diffraction for all d.

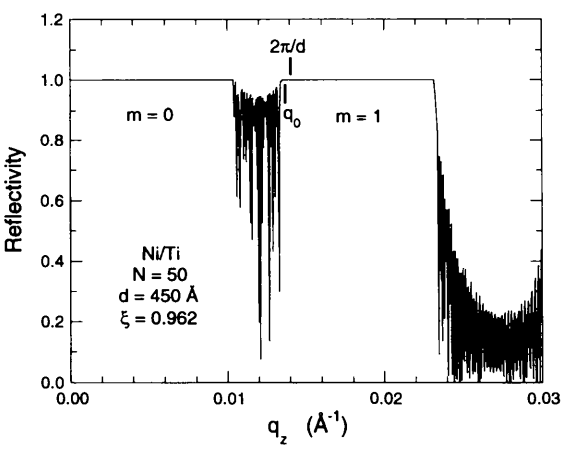

Fig. 7. Reflectivity of a periodic Ni/Ti multilayer as a function of q_z calculated exactly using the optical-matrix method. The dominant features are the mirror reflection ($m = 0$) and the first-order Bragg peak ($m = 1$). The vertical lines indicate the positions of the reciprocal-lattice vector $2\pi/d$ and the small-d limit of the critical wave vector for mirror reflection q_0. The actual critical wave vector for mirror reflection is depressed owing to the interaction with the Bragg peak at this large value of d (see text).

In general, it follows from the definitions (20) and (38) and expression (60) for the structure factor of a symmetric bilayer that the condition (52) is equivalent to

$$|(f_A - f_B)/(f_A + f_B)| \geq \pi/4. \quad (53)$$

This condition is always satisfied if, as in Ni/Ti, the scattering-length densities f_A and f_B are of opposite sign. If they have the same sign then (52) will be satisfied only if one is roughly an order of magnitude larger than the other, which is not the case for Fe/Ge.

Finally, it will be noted from Fig. 7 that the small gap between the mirror reflection ($m = 0$) and the Bragg peak ($m = 1$) can be filled in by introducing a suitable gradient in the bilayer thickness d. One then obtains a so-called supermirror (Mezei, 1976; Mezei & Dagleish, 1977; Hayter & Mook, 1989).

5.3. *Scaling laws*

The relation (47) for the position of the center of the Darwin plateau can be expressed equivalently as

$$Q_m/q_0 = K_m/q_0 + q_0/2K_m, \quad (54)$$

which demonstrates that Q_m/q_0 is a universal function of K_m/q_0. This scaling law is shown by the solid curve in Fig. 8. The results are displayed on a log–log scale to enhance the discrepancies at small K_m. The dashed line is the corresponding result ($Q_m = K_m$) from the kinematical theory of diffraction. The symbols in Fig. 8 show the values calculated from the optical-matrix method for Ni/Ti and Fe/Ge multilayers for various values of d and m. These exact values are in good agreement with (54) for $K_m > 2q_0$, which means $\xi < 0.25$. When K_m falls below this value, the expansion parameter ξ is no longer small in comparison with unity and the dynamical theory of diffraction begins to break down.

The relation (48) for the width of the Darwin plateau can be expressed equivalently as

$$\Delta Q_m/q_m = q_m/K_m, \quad (55)$$

which demonstrates that $\Delta Q_m/q_m$ is a universal function of K_m/q_m. This scaling law is shown, again on a log–log scale, by the solid line in Fig. 9. The symbols show the values calculated from the optical-matrix method for Ni/Ti and Fe/Ge multilayers for various values of d and m. These exact values are in good agreement with (55) for $K_m > 10q_m$, say. When K_m falls below this value, the Darwin plateau is slightly narrower than is predicted by the dynamical theory of diffraction.

APPENDIX A
Structure factors

In this Appendix, we derive explicit expressions for the structure factors for some model bilayers (Sears, 1983). In general,

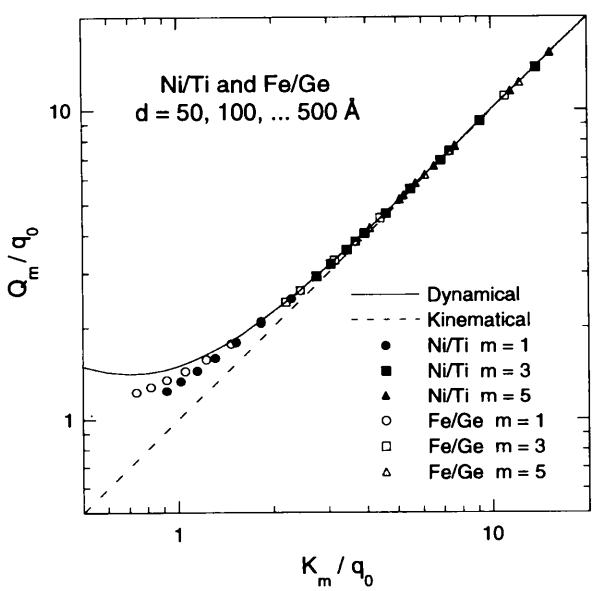

Fig. 8. Universal scaling law for Q_m, the position of the center of the Darwin plateau. The solid curve is from the dynamical theory of diffraction, the dashed line from the kinematical theory of diffraction and the symbols are exact values calculated from the optical-matrix method for Ni/Ti and Fe/Ge multilayers for various values of d and m.

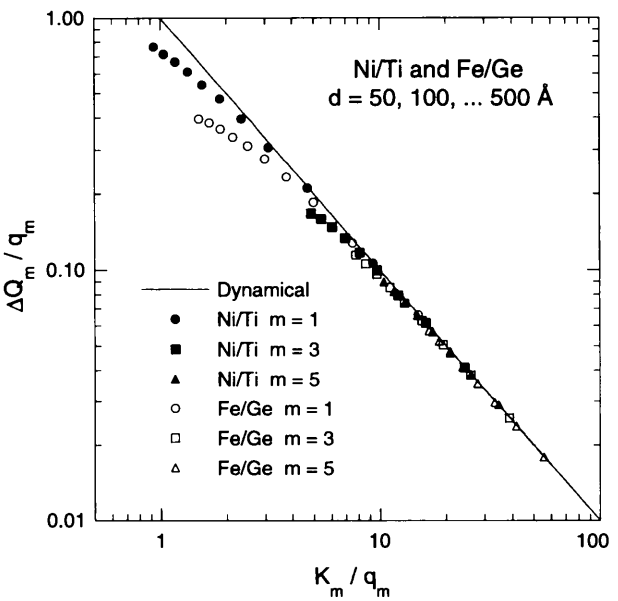

Fig. 9. Universal scaling law for ΔQ_m, the width of the Darwin plateau. The solid line is from the dynamical theory of diffraction, and the symbols are exact values calculated from the optical-matrix method for Ni/Ti and Fe/Ge multilayers for various values of d and m.

$$f_m = (1/d)\int_0^d \exp(iK_m z) f(z)\,dz. \tag{56}$$

Note that $f_{-m} = f_m^*$ for a non-absorbing bilayer where $f(z)$ is real. This is the analog of Friedel's law (Friedel, 1913). Note too that f_0 is the average value of $f(z)$,

$$f_0 = (1/d)\int_0^d f(z)\,dz. \tag{57}$$

For a general bilayer, in which the layers are labeled A and B,

$$f(z) = \begin{cases} f_A, & 0 < z < sd, \\ f_B, & sd < z < d, \end{cases} \tag{58}$$

where $f_A = \rho_A b_A$, $f_B = \rho_B b_B$ and s is the relative thickness of the A layer. This then gives

$$f_m = \begin{cases} sf_A + (1-s)f_B, & m = 0, \\ (f_A - f_B)\{[\exp(2sm\pi i) - 1]/2m\pi i\}, & m \neq 0. \end{cases} \tag{59}$$

If the bilayer is symmetric in the sense that the A and B layers are of equal thickness, then $s = 1/2$ and

$$f_m = \begin{cases} \frac{1}{2}(f_A + f_B), & m = 0, \\ (i/m\pi)(f_A - f_B), & m = \pm 1, \pm 3, \ldots, \\ 0, & m = \pm 2, \pm 4, \ldots. \end{cases} \tag{60}$$

Thus, the even-order reflections are all forbidden for a symmetric bilayer (Schoenborn, Caspar & Kammerer, 1974; Saxena & Schoenborn, 1975).

The dynamical theory of diffraction does not require an ideal multilayer (*i.e.* a sequence of homogeneous layers separated by plane-parallel boundaries). It is only necessary that the scattering-length density $f(z)$ be a periodic function of z. Thus, the dynamical theory can easily allow for the fact that, in reality, the boundaries between the layers are always smoothed out to some extent by diffusion and interlayer roughness. In the extreme case where the effective scattering-length density varies sinusoidally with z, we have

$$f(z) = \tfrac{1}{2}[(f_A + f_B) + (f_A - f_B)\sin(2\pi z/d)] \tag{61}$$

and

$$f_m = \begin{cases} \frac{1}{2}(f_A + f_B), & m = 0, \\ \pm(i/4)(f_A - f_B), & m = \pm 1, \\ 0, & m = \pm 2, \pm 3, \ldots. \end{cases} \tag{62}$$

In this case, all the higher-order reflections are forbidden.

APPENDIX B
Mirror reflection

In this Appendix, we derive the basic formula (31) for mirror reflection from a multilayer. We begin by supposing that Bragg's law is not satisfied, so that $q_z \neq K_m$ for any $m \neq 0$. It then follows from §2.3 that

$$D_m = \begin{cases} O(\xi), & m = 0, \\ O(1), & m \neq 0 \end{cases} \tag{63}$$

and, hence, that

$$A_m = \begin{cases} O(1), & m = 0, \\ O(\xi), & m \neq 0. \end{cases} \tag{64}$$

For each allowed value of K_z, the interior wave function (15) is then given by

$$\chi(z) = A_0 \exp(iK_z z) + O(\xi). \tag{65}$$

The allowed values of K_z are determined from (16), which reduces for $m = 0$ to

$$D_0 A_0 = \xi A_0 + O(\xi^2). \tag{66}$$

To lowest order in ξ this gives

$$D_0 = 1 - (K_z/k_z)^2 = \xi. \tag{67}$$

The allowed wave vectors are therefore $\pm K_z$, where

$$K_z/k_z = n_z = (1 - \xi)^{1/2}. \tag{68}$$

The quantity n_z is similar to an index of refraction.

To lowest order in ξ, the complete interior wave function is therefore of the form

$$\chi(z) = A_0 \exp(iK_z z) + A_0' \exp(-iK_z z), \tag{69}$$

in which the first term is the transmitted wave and the second term the wave reflected from the back face of the multilayer. Thus, when Bragg's law is not satisfied, the interior wave function in a multilayer is the same as in a single homogeneous layer of thickness D and scattering-length density f_0.

It follows from (12) and (69) that the requirement that $\chi(z)$ and $\chi'(z)$ be continuous at $z = 0$ and $z = D$ leads to four linear equations that can be solved for the amplitudes A_0, A_0', r and t. In particular, we find that the amplitude of the exterior reflected wave is given by Airy's formula (Born & Wolf, 1975):

$$r = -\frac{\alpha[1 - \exp(2i\varphi)]}{1 - \alpha^2 \exp(2i\varphi)}, \tag{70}$$

in which

$$\alpha = (n_z - 1)/(n_z + 1) \tag{71}$$

and

$$\varphi = q_z n_z D/2. \tag{72}$$

The result (70) can be expressed equivalently as

$$r = \frac{1 - n_z^2}{1 + n_z^2 + 2in_z \cot\varphi}. \tag{73}$$

It is convenient to introduce the dimensionless variables

$$x = q_z/q_0, \quad y = q_0 D/2, \tag{74}$$

in which case

$$r = \{2x^2 - 1 + 2ix(x^2-1)^{1/2}\cot[y(x^2-1)^{1/2}]\}^{-1} \tag{75}$$

and the reflectivity is then given according to (13) by

$$R_0(x,y) = \left|2x^2 - 1 + 2ix(x^2-1)^{1/2}\cot[y(x^2-1)^{1/2}]\right|^{-2}, \tag{76}$$

which is the desired result (31).

APPENDIX C
Bragg reflection

In this Appendix, we derive the basic formula (41) for Bragg reflection from a multilayer. We begin by supposing that Bragg's law is satisfied in the sense that $q_z \simeq K_m$ for some value of $m \neq 0$. It then follows from §2.3 that

$$D_{m'} = \begin{cases} O(\xi), & m' = 0, m, \\ O(1), & \text{otherwise} \end{cases} \tag{77}$$

and, hence, that

$$A_{m'} = \begin{cases} O(1), & m' = 0, m, \\ O(\xi), & \text{otherwise.} \end{cases} \tag{78}$$

For each allowed value of K_z, the interior wave function (15) is then given by

$$\chi(z) = A_0 \exp(iK_z z) + A_m \exp[i(K_z - K_m)z] + O(\xi). \tag{79}$$

The amplitudes are determined from equations (16), which now become

$$\begin{aligned} D_0 A_0 &= \xi(\hat{f}_0 A_0 + \hat{f}_{-m} A_m) + O(\xi^2), \\ D_m A_m &= \xi(\hat{f}_m A_0 + \hat{f}_0 A_m) + O(\xi^2). \end{aligned} \tag{80}$$

Recalling that $\hat{f}_0 = 1$, and keeping only the leading terms in ξ, we get

$$\begin{aligned} (D_0 - \xi)A_0 - \xi\hat{f}_{-m}A_m &= 0, \\ -\xi\hat{f}_m A_0 + (D_m - \xi)A_m &= 0. \end{aligned} \tag{81}$$

These homogeneous linear equations have a solution only if the determinant of the coefficients vanishes,

$$(D_0 - \xi)(D_m - \xi) = \xi^2 \hat{f}_m \hat{f}_{-m}, \tag{82}$$

and this relation then determines the allowed values of K_z. The solution of the equations (81) is then given by

$$X \equiv \frac{A_m}{A_0} = \frac{D_0 - \xi}{\xi\hat{f}_{-m}} = \frac{\xi\hat{f}_m}{D_m - \xi}. \tag{83}$$

Again, keeping only the leading terms in ξ, the interior wave function (79) now becomes

$$\chi(z) = A_0[\exp(iK_z z) + X\exp(-iK'_z z)], \tag{84}$$

in which

$$K'_z = K_m - K_z. \tag{85}$$

Thus, for each allowed value of K_z, the interior wave function is the sum of a transmitted wave (with wave vector K_z) and a Bragg-reflected wave (with wave vector $-K'_z$).

Let us write the relations (17) in the form

$$\begin{aligned} D_0 &= 1 - (K_z/k_z)^2 = \xi p, \\ D_m &= 1 - (K'_z/k_z)^2 = \xi p', \end{aligned} \tag{86}$$

so that

$$\begin{aligned} K_z/k_z &= n_z = (1 - \xi p)^{1/2} \\ K'_z/k_z &= n'_z = (1 - \xi p')^{1/2}. \end{aligned} \tag{87}$$

Then, (82) becomes

$$(p-1)(p'-1) = \beta, \tag{88}$$

where

$$\beta = \hat{f}_m \hat{f}_{-m}. \tag{89}$$

Also, (85) shows that, to first order in ξ,

$$p + p' = (2/\xi)(2 - K_m/k_z) \equiv 2\alpha. \tag{90}$$

Hence, (88) becomes a quadratic equation in p,

$$(p-1)(2\alpha - p - 1) = \beta, \tag{91}$$

with roots

$$p_\pm = \alpha \pm [(\alpha - 1)^2 - \beta]^{1/2}. \tag{92}$$

The indices of refraction n_z and n'_z are therefore both double valued and the complete interior wave function becomes

$$\begin{aligned} \chi(z) = A_+[\exp(iK_{z+}z) + X_+\exp(-iK'_{z+}z)] \\ + A_-[\exp(iK_{z-}z) + X_-\exp(-iK'_{z-}z)], \end{aligned} \tag{93}$$

in which, to first order in ξ,

$$\begin{aligned} K_{z\pm} &= k_z(1 - \xi p_\pm/2), \\ K'_{z\pm} &= K_m - K_{z\pm}, \\ X_\pm &= (p_\pm - 1)\hat{f}_{-m}. \end{aligned} \tag{94}$$

The physical content of the wave function (93) becomes clearer when the terms are regrouped as

$$\begin{aligned} \chi(z) = [A_+\exp(iK_{z+}z) + A_-\exp(iK_{z-}z)] \\ + [A_+X_+\exp(-iK'_{z+}z) + A_-X_-\exp(-iK'_{z-}z)]. \end{aligned} \tag{95}$$

Then the first two terms represent the interior transmitted wave, which, since n_z is double valued, have slightly different wave vectors $K_{z\pm}$. The final two terms represent the interior Bragg-reflected wave, which, since n'_z is double valued, have slightly different wave vectors $-K'_{z\pm}$. The wave function (95) neglects

mirror reflection from the faces of the multilayer. This is justified by the fact that, when $q_z \simeq K_m$, the amplitudes of the mirror-reflected waves are of order ξ and hence of the same order as the other terms in $\chi(z)$ that have already been neglected. Thus, mirror reflection must also be neglected for consistency.

The amplitudes of the waves are determined by matching the transmitted and Bragg-reflected components of the interior wave function (95) to the corresponding components in the exterior wave function (12) at $z = 0$ and $z = D$. This gives

$$\begin{aligned} 1 &= A_+ + A_-, & t &= A_+Y_+ + A_-Y_-, \\ r &= A_+X_+ + A_-X_-, & 0 &= A_+X_+Y_+ + A_-X_-Y_-, \end{aligned} \tag{96}$$

in which

$$Y_\pm = \exp(-i\xi p_\pm k_z D/2). \tag{97}$$

Hence,

$$\begin{aligned} A_+ &= \frac{-X_-Y_-}{X_+Y_+ - X_-Y_-}, & r &= \frac{X_+X_-(Y_+ - Y_-)}{X_+Y_+ - X_-Y_-}, \\ A_- &= \frac{X_+Y_+}{X_+Y_+ - X_-Y_-}, & t &= \frac{Y_+Y_-(X_+ - X_-)}{X_+Y_+ - X_-Y_-}. \end{aligned} \tag{98}$$

The reflectivity and transmissivity are, in general, given by (13). In the case of zero absorption, where $\hat{f}_{-m} = \hat{f}_m^*$ and $\beta = |\hat{f}_m|^2$, we find after a little algebra that

$$R + T = 1, \tag{99}$$

as it should for neutron conservation. The reflectivity is found to be of the form (Ewald, 1917)

$$R(x, y) = \frac{\sin^2[y(x^2 - 1)^{1/2}]}{x^2 - 1 + \sin^2[y(x^2 - 1)^{1/2}]}, \tag{100}$$

in which the dimensionless variables x and y are now defined such that

$$x^2 = (\alpha - 1)^2/\beta, \quad y^2 = \beta(\xi k_z D/2)^2. \tag{101}$$

The signs of x and y are arbitrary since $R(x, y)$ is an even function of these variables. It follows from (89) and (90) that

$$x = [2K_m(q_z - K_m) - q_0^2]/q_m^2, \quad y = q_m^2 D/4K_m, \tag{102}$$

where q_0 is given by (20) and

$$q_m^2 = 16\pi|f_m|. \tag{103}$$

Expression (100) for the reflectivity is the desired result (41).

References

Abelès, F. (1948). *Ann. Phys. (Paris)*, **3**, 504–520.

Born, M. & Wolf, E. (1975). *Principles of Optics*, 5th ed. Oxford: Pergamon.

Darwin, C. G. (1914). *Philos. Mag.* **27**, 315–333, 675–690.

Ebisawa, T., Achiwa, N., Yamada, S., Akiyoshi, T. & Okamoto, S. (1979). *J. Nucl. Sci. Tech.* **16**, 647–659.

Ewald, P. P. (1917). *Ann. Phys. (Leipzig)*, **54**, 519–556, 557–597.

Friedel, G. (1913). *C. R. Acad. Sci.* **157**, 1533–1536.

Gukasov, A. G., Deriglazov, V. V., Kezerashvilli, V. Ya., Krutov, G. A., Kudryashov, V. A., Peskov, B. G., Syromyatnikov, V. G., Trunov, V. A., Kharchenkov, V. P. & Shchebetov, A. F. (1979). *Sov. Phys. JETP*, **50**, 862–865.

Hayter, J. B. & Mook, H. A. (1989). *J. Appl. Cryst.* **22**, 35–41.

Heavens, O. S. (1965). *Optical Properties of Thin Solid Films*. New York: Dover.

Jacobsson, R. (1966). *Prog. Optics*, **5**, 247–286.

Laue, M. von (1931). *Ergeb. Exakten Naturwiss.* **10**, 133–158.

Lekner, J. (1987). *Theory of Reflection of Electromagnetic and Particle Waves*. Dordrecht: Nijhoff-Kluwer.

Mezei, F. (1976). *Commun. Phys.* **1**, 81–85.

Mezei, F. & Dagleish, P. A. (1977). *Commun. Phys.* **2**, 41–43.

Renninger, M. (1937). *Z. Phys.* **106**, 141–176.

Saxena, A. M. (1986). *J. Appl. Cryst.* **19**, 123–130.

Saxena, A. M. & Schoenborn, B. P. (1975). *Neutron Scattering for the Analysis of Biological Structures*, edited by B. P. Schoenborn. Report BNL 50453, Chapter VII, pp. 30–47. Brookhaven National Laboratory, USA.

Saxena, A. M. & Schoenborn, B. P. (1977). *Acta Cryst.* A**33**, 805–813.

Schoenborn, B. P., Caspar, D. L. D. & Kammerer, O. F. (1974). *J. Appl. Cryst.* **7**, 508–510.

Sears, V. F. (1983). *Acta Cryst.* A**39**, 601–608.

Sears, V. F. (1988). *Thin-Film Neutron Optical Devices*, edited by C. F. Majkrzak. *SPIE Proc.* **983**, 193–198.

Sears, V. F. (1989). *Neutron Optics*. New York: Oxford University Press.

Zachariasen, W. H. (1945). *Theory of X-ray Diffraction in Crystals*. New York: Wiley.